Quantum Electrodynamics and Quantum Optics: Lecture 9

Fall 2025

Single two level system as mirror

Demonstration of a Single-Photon Router in the Microwave Regime

Io-Chun Hoi,[1] C. M. Wilson,[1] Göran Johansson,[1] Tauno Palomaki,[1] Borja Peropadre,[2] and Per Delsing[1]

[1]*MC2, Chalmers University of Technology, Göteborg, Sweden*

[2]*Instituto de Física Fundamental Serrano, CSIC, Madrid, Spain*

(Received 21 February 2011; revised manuscript received 4 June 2011; published 9 August 2011)

We have embedded an artificial atom, a superconducting transmon qubit, in an open transmission line and investigated the strong scattering of incident microwave photons ($\sim$6 GHz). When an input coherent state, with an average photon number $N \ll 1$ is on resonance with the artificial atom, we observe extinction of up to 99.6% in the forward propagating field. We use two-tone spectroscopy to study scattering from excited states and we observe electromagnetically induced transparency (EIT). We then use EIT to make a single-photon router, where we can control to what output port an incoming signal is delivered. The maximum on-off ratio is around 99% with a rise and fall time on the order of nanoseconds, consistent with theoretical expectations. The router can easily be extended to have multiple output ports and it can be viewed as a rudimentary quantum node, an important step towards building quantum information networks.

DOI: 10.1103/PhysRevLett.107.073601 PACS numbers: 42.50.Gy, 03.67.Hk, 85.25.Cp

Single two level system as mirror

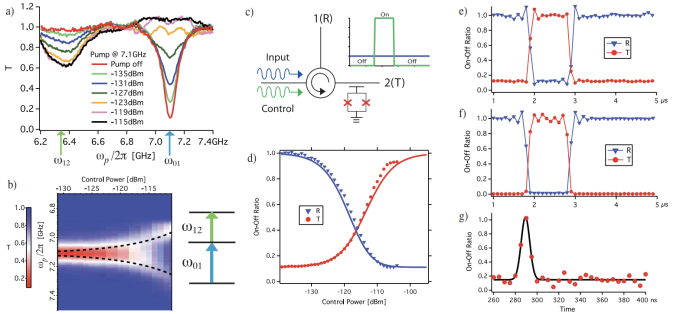

FIG. 2 (color online). (a) Two-tone spectroscopy of sample 1. A microwave pump is continuously applied at ω_{01} with increasing power while a weak probe tone is swept in frequency. As the population in the first state is increased, due to the drive at ω_{01}, scattering at ω_{12} becomes possible, appearing as another dip in the transmittance. From this, we extract $\omega_{12}/2\pi = 6.38$ GHz. (b) The microwave pump is now applied at ω_{12}. As the power of the ω_{12} pump increases, we see electromagnetically induced transparency (EIT) at ω_{01} as the Autler-Townes doublet splits with a separation equal to the Rabi frequency $\Omega_c/2\pi$ (black dashed lines). (inset) Energy level diagram. (c) Cartoon of the router. With the control off, the input probe is reflected from the transmon, and is routed to port 1 through the circulator. When the control is on, the input is transmitted to port 2. Inset: the control pulse sequence. (d) Normalized on-off ratio (see text) of the transmittance (T) and reflectance (R) as a function of control pulse power, measured simultaneously on sample 1. The symbols are the data and the solid lines are fits. (e) Time dependence of T and R at ω_{01}, measured simultaneously for sample 1, while a control pulse is applied. (f) Same for sample 2, although T and R are measured separately. We see that the input signal is routed with an on-off ratio of $\sim$90% ($\sim$ 99%) for sample 1 (2). (g) The response of sample 1 to a 10 ns Gaussian control pulse (circles), along with a Gaussian fit (solid line). We see that the transmittance smoothly follows the control on the few ns time scale while maintaining the high on-off ratio.

Explanation on how absorption works

Stimulated emission from single quantum dipoles

Kerry J Vahala

Department of Applied Physics, Mail Stop 128-95, California Institute of Technology, Pasadena, CA 91125, USA

Received 9 November 1992

Abstract. Whereas the basic features of stimulated emission are easily seen to hold true for ensembles of dipoles, the same is not always true for a single dipole system. For example, symmetry requires that well localized, bound dipoles emit a dipole field which is isotropic in the plane defined by the dipole vector. Indeed, for this case, nothing in the interaction between the dipole and the field contains information on the propagation direction of the field. These observations seem at odds with the highly directional nature of stimulated emission. We therefore test for stimulated emission by an explicit calculation considering both a single Rabi type dipole and a damped dipole whose centre-of-mass coordinates are fixed at a point. Remarkably, despite the symmetrical dipole radiation pattern, stimulated emission into the original stimulating wave is shown to occur exactly. An explanation of this effect is then considered by investigating dipoles whose centre-of-mass coordinates are allowed to vary. In this case, photon recoil of the dipole introduces a directional sense to the interaction. In the extreme opposite and trivial case of a highly delocalized dipole (centre-of-mass momentum eigenstates) stimulated emission again occurs exactly. In all intermediate cases, however, stimulated emission occurs only partially or approximately. A condition imposed on a dipole's spatial extent is established for stimulated emission to occur approximately. Finally, the original bound and localized dipole is seen to be a special limiting case of recoiling dipoles for which stimulated emission occurs exactly.

Explanation on how absorption works: with single bound dipole

In the radiation zone, the total energy contained in the interference of the stimulating field and the dipole field is given by:

$$\Delta E_{\pm} = \varepsilon_0 \int_{\pm} r^2 \, \mathrm{d}r \, \mathrm{d}S 2 \boldsymbol{E}_{\mathrm{d}}(r, \theta, \phi) \cdot \boldsymbol{E}_0 \cos(\boldsymbol{k} \cdot \boldsymbol{r} - \omega t) \tag{5}$$

where $\mathrm{d}S$ is the differential solid angle and the integration is performed over the entire volume defined by a plus or a minus shell. After calculation the integral in (5) reduces to the form:

$$\Delta E_{\pm} = \pm \hbar \omega. \tag{6}$$

Thus, the stimulated photon is correctly added to the wave responsible for the stimulation, despite the fact that the atomic dipole has no indication of this wave's propagation direction.

Explanation on how absorption works: dipole with recoil

the dipole in the ground state and in the excited state, respectively. A well known result concerning the interaction of these states under resonant optical excitation is that only closed families of states interact. In the present case, only the ground and excited states for which $\boldsymbol{k}_2 - \boldsymbol{k}_1 = \boldsymbol{k}$ will interact where $\boldsymbol{k}$ is the optical wave vector. In deriving the equations of motion, this momentum selection rule is a direct consequence of the global nature of the interaction energy term in the Hamiltonian and the extended nature of both the atomic states and the optical plane wave. Combined with the assumption of resonant excitation, it is clear that stimulated emission into the correct optical mode is guaranteed by this selection rule. It is also clear that the absence of this same selection

Quantum Langevin Equation of open cavity

Cavity Hamiltonian

$$\hat{H} = \sum \underbrace{\hbar\omega_{k'}\hat{a}^{\dagger}{}_{k'}\hat{a}_{k'}}_{\text{cavity modes}} + \sum \hbar\omega_k \hat{b}_k^{\dagger}\hat{b}_k + \hbar \sum_{k,k'} \underbrace{g_{k,k'}(\hat{a}_{k'}\hat{b}_k^{\dagger} + \hat{b}_k\hat{a}^{\dagger}{}_{k'})}_{\text{coupling terms}}$$

Taking the continuity limit $\sum_k |g_k|^2 = \int \mathrm{d}\omega_k |g(\omega_k)|^2 D(\omega_k)$, we define the operators in the frequency domain $[\hat{b}(\omega), \hat{b}^{\dagger}(\omega')] = \delta(\omega - \omega')$, thus:

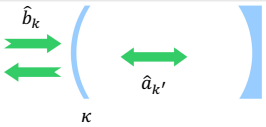

Equation of motion of $\hat{b}_k$

$$\frac{\mathrm{d}}{\mathrm{d}t}\hat{b}_k = -i\omega_k\hat{b}_k - ig_k\hat{a}$$

Forward and backward formal solutions

- For $t_0 < t$, meaning that the process is a forward noise input

$$\hat{b}_k = e^{-i\omega_k(t-t_0)}\hat{b}_k(t_0) - ig_k \int_{t_0}^{t} e^{-i\omega_k(t-t')}\hat{a}(t')\mathrm{d}t'$$

- We can also write the process backward with $t_1 > t$ as

$$\hat{b}_k = e^{-i\omega_k(t-t_1)}\hat{b}_k(t_1) + ig_k \int_{t}^{t_1} e^{-i\omega_k(t-t')}\hat{a}(t')\mathrm{d}t'.$$

Quantum Langevin Equation

How to derive

Going to the continuum $\sum_k \to \int \mathrm{d}\omega_k D(\omega_k)$, where $D(\omega_k)$ is the density of states (DOS), we can also derive from $\dot{\hat{a}} = -\frac{i}{\hbar}[\hat{a}, \hat{H}_{\mathrm{sys}}] - \sum_k g_k \hat{b}_k$ to (forward):

$$\begin{aligned}\dot{\hat{a}} =& -i\omega\hat{a} - i\sum_k g_k e^{-i\omega_k(t-t_0)}\hat{b}_k(t_0) \\ &- \int_{-\infty}^{+\infty} \mathrm{d}\omega_k |g(\omega_k)|^2 D(\omega_k) \int_{t_0}^{t} e^{-i\omega_k(t-t')}\hat{a}(t')\mathrm{d}t'\end{aligned}$$

- Assuming $|g(\omega_k)|^2 = |g|^2$ (first Markov approximation).
- Defining $2\pi|g|^2 D(\omega_k) = \kappa$ and $\hat{a}_{\mathrm{in}} = -i\sum_k g_k e^{-i\omega_k(t-t_0)} b_k(t_0)$.
- Noting that $\int_{-\infty}^{\infty} \frac{\mathrm{d}\omega}{2\pi} e^{-i\omega t} = \delta(t)$ and $\int_{t_0}^{t} \delta(t-t')f(t')\mathrm{d}t' = \frac{1}{2}f(t)$.

Forward and backward Quantum Langevin Equations

Quantum Langevin Equation (forward)

$$\dot{\hat{a}} = -i\omega\hat{a} - \frac{\kappa}{2}\hat{a} + \sqrt{\kappa}\hat{a}_{\text{in}}$$

$$[\hat{a}_{\text{in}}(t), \hat{a}^{\dagger}_{\text{in}}(t')] = \delta(t - t')$$

One can repeat the same analysis, but now for the **backward** evolution, with $\hat{a}_{\text{out}} = -i\sum_k g_k e^{-i\omega_k(t-t_1)} b_k(t_1)$ and get:

Quantum Langevin Equation (backward)

$$\dot{\hat{a}} = -i\omega\hat{a} + \frac{\kappa}{2}\hat{a} - \sqrt{\kappa}\hat{a}_{\text{out}}$$

Input Output Relation[1]

Subtracting the forward and backward Langevin Equations yields:

Input-output Noise Relation

$$\hat{a}_{\text{out}} + \hat{a}_{\text{in}} = \sqrt{\kappa}\hat{a}$$

Note that from the photon number point of view κ represents the energy decay:

$$\frac{d}{dt}\langle\hat{n}\rangle = \frac{d}{dt}\langle\hat{a}^\dagger\hat{a}\rangle = -\kappa\langle\hat{a}^\dagger\hat{a}\rangle + \langle\hat{a}_{\text{in}}^\dagger\hat{a}_{\text{in}}\rangle$$

[1] Walls, D. F., Milburn, G. J. "Quantum optics" (2007). Chapter 7

Application : Transmission & Reflection

We can first write down the quantum Langevin equations

$$\partial_t \begin{pmatrix} \hat{a} \\ \hat{a}^\dagger \end{pmatrix} = \begin{pmatrix} -i\omega_c - \kappa/2 & 0 \\ 0 & i\omega_c - \kappa/2 \end{pmatrix} \begin{pmatrix} \hat{a} \\ \hat{a}^\dagger \end{pmatrix} + \sqrt{\kappa} \begin{pmatrix} \hat{a}_{\text{in}} \\ \hat{a}_{\text{in}}^\dagger \end{pmatrix}$$

where $\hat{a}^\dagger(\omega) = [\hat{a}(\omega)]^\dagger$ and solve in the Fourier domain

$$i\omega \begin{pmatrix} \hat{a}(\omega) \\ \hat{a}^\dagger(\omega) \end{pmatrix} = \underbrace{\begin{pmatrix} -i\omega_c - \kappa/2 & 0 \\ 0 & i\omega_c - \kappa/2 \end{pmatrix}}_{\hat{M}} \begin{pmatrix} \hat{a} \\ \hat{a}^\dagger \end{pmatrix} + \sqrt{\kappa} \begin{pmatrix} \hat{a}_{\text{in}}(\omega) \\ \hat{a}_{\text{in}}^\dagger(\omega) \end{pmatrix}$$

$$\Rightarrow \begin{pmatrix} \hat{a}(\omega) \\ \hat{a}^\dagger(\omega) \end{pmatrix} = \sqrt{\kappa}[-\hat{M} + i\omega\hat{\mathbb{1}}]^{-1} \begin{pmatrix} \hat{a}_{\text{in}}(\omega) \\ \hat{a}_{\text{in}}^\dagger(\omega) \end{pmatrix}$$

Application : Transmission & Reflection

Cavity transmission / reflection

$$\hat{a}_{\text{out}}(\omega) = \frac{\kappa/2 + i(\omega - \omega_c)}{\kappa/2 - i(\omega - \omega_c)} \hat{a}_{\text{in}}(\omega)$$

$$T(\omega) = \frac{\langle \hat{a}^\dagger_{\text{out}}(\omega) \hat{a}_{\text{out}}(\omega) \rangle}{\langle \hat{a}^\dagger_{\text{in}}(\omega) \hat{a}_{\text{in}}(\omega) \rangle}$$

Here we plot the phase of the transmission.

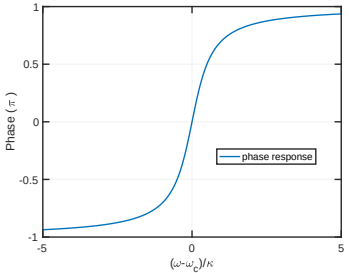

Separating intrinsic and external loss

The decay κ modeled is very general, the following showcases how to introduce intrinsic and external losses into the equations as $\kappa = \kappa_{\mathrm{ex}} + \kappa_{\mathrm{in}}$.

Modified Quantum Langevin Equation (forward)

$$\dot{\hat{a}} = -i\omega\hat{a} - \frac{\kappa_{\mathrm{ex}} + \kappa_{\mathrm{in}}}{2}\hat{a} + \sqrt{\kappa_{\mathrm{ex}}}\hat{a}_{\mathrm{in}} + \sqrt{\kappa_{\mathrm{in}}}\hat{f}_{\mathrm{in}}$$

$$[\hat{a}_{\mathrm{in}}(t), \hat{a}^{\dagger}_{\mathrm{in}}(t')] = \delta(t - t')$$

$$[\hat{f}_{\mathrm{in}}(t), \hat{f}^{\dagger}_{\mathrm{in}}(t')] = \delta(t - t')$$

Modified Cavity transmission / reflection

$$\hat{a}_{\mathrm{out}}(\omega) = \frac{(\kappa_{\mathrm{ex}} - \kappa_{\mathrm{in}})/2 + i(\omega - \omega_c)}{(\kappa_{\mathrm{ex}} + \kappa_{\mathrm{in}})/2 - i(\omega - \omega_c)}\hat{a}_{\mathrm{in}}(\omega)$$

Purcell Effect in Spontaneous Emission

$$\hat{H} = \sum \hbar\omega_k' \hat{a}^\dagger \hat{a} + \frac{\hbar\omega}{2}\hat{\sigma}_z + \hbar g(\hat{\sigma}^+ \hat{a} + \hat{\sigma}^- \hat{a}^\dagger) + \sum \hbar\omega_k \hat{b}_k^\dagger \hat{b}_k + \sum_k g_k(\hat{a}\hat{b}_k^\dagger + \hat{b}_k \hat{a}^\dagger)$$

Approximate treatment yields the spontaneous decay rate

$$\Gamma_c = \frac{4}{3\kappa}\frac{|P_{12}|^2\omega}{2\hbar\epsilon_0 V} \propto 2\pi|g|^2\rho(\omega) \propto 2\pi|g|^2 F_{\text{Purcell}}\rho_{\text{free space}}$$

and the density of state $\rho(\omega)$ of resonator is

$$\rho(\omega) = \frac{1}{\pi}\frac{\kappa/2}{(\omega-\omega_c)^2 + (\kappa/2)^2}\frac{1}{V}.$$

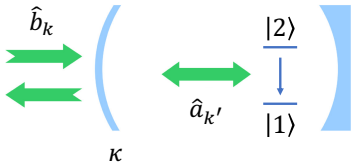

Purcell Effect in Spontaneous Emission

The Purcell factor expressed as the Quality factor (Q) and the Mode Volume of the cavity (V)

$$\Gamma_c = \Gamma_0 \cdot \frac{3Q}{4V} \cdot \lambda^3$$

B10. Spontaneous Emission Probabilities at Radio Frequencies. E. M. PURCELL, *Harvard University*.—For nuclear magnetic moment transitions at radio frequencies the probability of spontaneous emission, computed from

$$A_\nu = (8\pi\nu^2/c^3)h\nu(8\pi^3\mu^2/3h^2) \text{ sec.}^{-1},$$

is so small that this process is not effective in bringing a spin system into thermal equilibrium with its surroundings. At 300°K, for $\nu = 10^7$ sec.$^{-1}$, $\mu = 1$ nuclear magneton, the corresponding relaxation time would be 5×10^{21} seconds! However, for a system coupled to a resonant electrical circuit, the factor $8\pi\nu^2/c^3$ no longer gives correctly the number of radiation oscillators per unit volume, in unit frequency range, there being now *one* oscillator in the frequency range ν/Q associated with the circuit. The spontaneous emission probability is thereby increased, and the relaxation time reduced, by a factor $f = 3Q\lambda^3/4\pi^2V$, where V is the volume of the resonator. If a is a dimension characteristic of the circuit so that $V \sim a^3$, and if δ is the skin-depth at frequency ν, $f \sim \lambda^3/a^2\delta$. For a non-resonant circuit $f \sim \lambda^3/a^3$, and for $a < \delta$ it can be shown that $f \sim \lambda^3/a\delta^2$. If small metallic particles, of diameter 10^{-3} cm are mixed with a nuclear-magnetic medium at room temperature, spontaneous emission should establish thermal equilibrium in a time of the order of minutes, for $\nu = 10^7$ sec.$^{-1}$.

Purcell Effect in Spontaneous Emission

Notice that the Purcell effect is an effect that is due to the enhancement of the mode density. The mode density can also be modified to inhibit spontaneous emission by trapping an electron in a Penning trap with dimension comparable to the emission wavelength[2]. One can compute the equations of motion[3] for $\langle \hat{a}^\dagger \hat{a} \rangle$ and $\langle \sigma_z \rangle$:

$$\frac{d}{dt}\langle \hat{a}^\dagger \hat{a} \rangle = -ig\langle \sigma_+ \hat{a} - \hat{a}^\dagger \sigma_- \rangle - \kappa \langle \hat{a}^\dagger \hat{a} \rangle + \kappa \underbrace{\overline{n}_{\text{th}}}_{\approx 0}$$

$$\frac{d}{dt}\langle \sigma_z \rangle = -ig\langle \sigma_+ \hat{a} - \hat{a}^\dagger \sigma_- \rangle$$

Notice that the average of the operator $\langle \sigma_+ \hat{a} - \hat{a}^\dagger \sigma_- \rangle$ has its equation of motion involving the quantity $\langle \hat{a}^\dagger \sigma_z \hat{a} \rangle$. In general, we get an infinite set of equations which may not be analytically solvable, but can be considerably simplified if initially the atom is in the excited state and the field inside the cavity is in the vacuum state.

[2] Gabrielse,Gerald,and Hans Dehmelt. "Observation of inhibited spontaneous emission." Physical review letters 55.1 (1985): 67.

[3] Scully, M.O., Zubairy, M.S. "Quantum optics" (1999). Chapter 9, Section 5

Purcell Effect in Spontaneous Emission: Example[4]

VOLUME 50, NUMBER 24 PHYSICAL REVIEW LETTERS 13 JUNE 1983

Observation of Cavity-Enhanced Single-Atom Spontaneous Emission

P. Goy, J. M. Raimond, M. Gross, and S. Haroche
Laboratoire de Physique de l'Ecole Normale Supérieure, F-75231 Paris Cedex 05, France

(Received 1 April 1983)

It has been observed that the spontaneous-emission lifetime of Rydberg atoms is shortened by a large ratio when these atoms are crossing a high-Q superconducting cavity tuned to resonance with a millimeter-wave transition between adjacent Rydberg states.

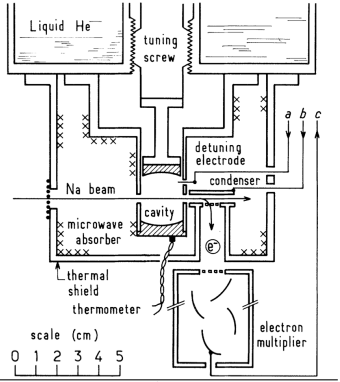

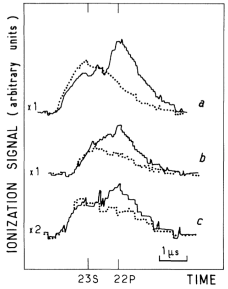

FIG. 3. Cavity-enhanced spontaneous emission signals. Dotted line, off-resonant cavity; full line, resonant cavity. The average numbers of atoms in the cavity are respectively 3.5, 2, and 1.3 in traces a, b, and c. Traces a and c correspond to $23S \rightarrow 22P_{3/2}$, trace b to $23S \rightarrow 22P_{1/2}$.

[4] Goy,Ph,et al.'Observation of cavity-enhanced single-atom spontaneous emission." Phys. Rev. Lett. 50,24 (1983): 1903.

Purcell Effect in Spontaneous Emission: Example[5]

VOLUME 83, NUMBER 7 PHYSICAL REVIEW LETTERS 16 AUGUST 1999

Observing the Quantum Limit of an Electron Cyclotron: QND Measurements of Quantum Jumps between Fock States

S. Peil and G. Gabrielse
Department of Physics, Harvard University, Cambridge, Massachusetts 02138
(Received 18 March 1999)

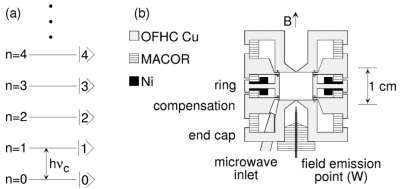

FIG. 1. (a) Energy levels of the one-electron cyclotron oscillator. (b) Electrodes of the cylindrical Penning trap cavity.

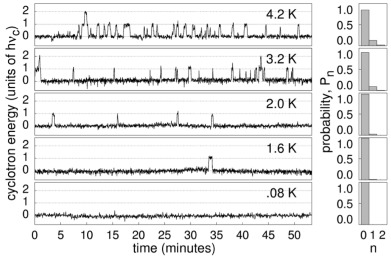

FIG. 2. Quantum jumps between the lowest states of the one-electron cyclotron oscillator decrease in frequency as the cavity temperature is lowered.

[5] Peil, S., and G. Gabrielse. "Observing the quantum limit of an electron cyclotron: QND measurements of quantum jumps between Fock states." Phys. Rev. Lett. 83.7 (1999): 1287.

Sythesizing arbitary quantum states in superconducting resonator

nature Vol 459|28 May 2009|doi:10.1038/nature08005

LETTERS

Synthesizing arbitrary quantum states in a superconducting resonator

Max Hofheinz[1], H. Wang[1], M. Ansmann[1], Radoslaw C. Bialczak[1], Erik Lucero[1], M. Neeley[1], A. D. O'Connell[1], D. Sank[1], J. Wenner[1], John M. Martinis[1] & A. N. Cleland[1]

Sythesizing arbitary quantum states in superconducting resonator

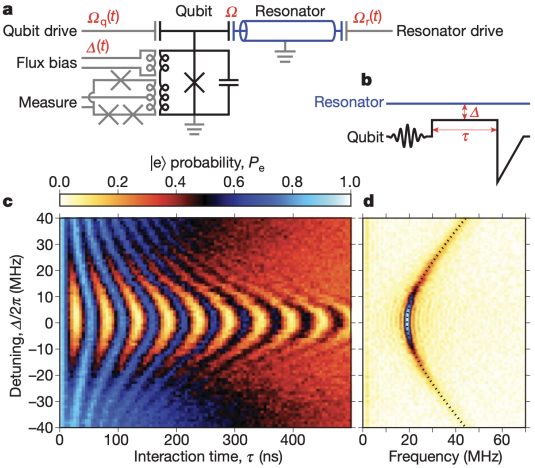

Sythesizing arbitary quantum states in superconducting resonator

Table 1 | Sequence to generate the resonator state $|\psi\rangle = |1\rangle + i|3\rangle$

Sequence of states, operations	Operational parameter	System state, parameter value
$\|\boldsymbol{\psi}\rangle$		$\|\boldsymbol{g}\rangle(\mathbf{0.707}\|1\rangle+\mathbf{0.707}\boldsymbol{i}\|3\rangle)$
S_3	$\tau_3\Omega$	1.81
Q_3	q_3	3.14
$\|\boldsymbol{\psi_2}\rangle$		$\|\boldsymbol{g}\rangle(-\mathbf{0.557}\boldsymbol{i}\|0\rangle+\mathbf{0.707}\|2\rangle)+\mathbf{0.436}\|e\rangle\|1\rangle$
Z_2	$t_2\Delta$	4.71
S_2	$\tau_2\Omega$	1.44
Q_2	q_2	$-2.09 - 2.34i$
$\|\boldsymbol{\psi_1}\rangle$		$(\mathbf{0.553}-\mathbf{0.62}\boldsymbol{i})\|g\rangle\|1\rangle-(\mathbf{0.371}+\mathbf{0.416}\boldsymbol{i})\|e\rangle\|0\rangle$
Z_1	$t_1\Delta$	3.26
S_1	$\tau_1\Omega$	1.96
Q_1	q_1	$-2.71-1.59i$
$\|\boldsymbol{\psi_0}\rangle$		$(\mathbf{0.197}-\mathbf{0.98}\boldsymbol{i})\|g\rangle\|0\rangle$

This resonator state is used for the measurements described in Fig. 2. The sequence is computed top to bottom, but applied bottom to top. The area and phase for the *n*th qubit drive Q_n is $q_n = \int \Omega_Q(t)e^{i\Delta_{ef}t}dt$ ($t = 0$ being the time when the qubit is tuned into resonance directly after the step Q_n), the time on-resonance for the qubit–resonator swap operation S_n is τ_n, and the time off-resonance (mod $2\pi/\Delta$) for the phase rotation Z_n is t_n. We note that the initial state $|\psi_0\rangle$ differs by an overall phase factor from the ground state $|g\rangle\,|0\rangle$, but this is not detectable. State descriptions are shown bold; operations are not in bold.

Sythesizing arbitary quantum states in superconducting resonator

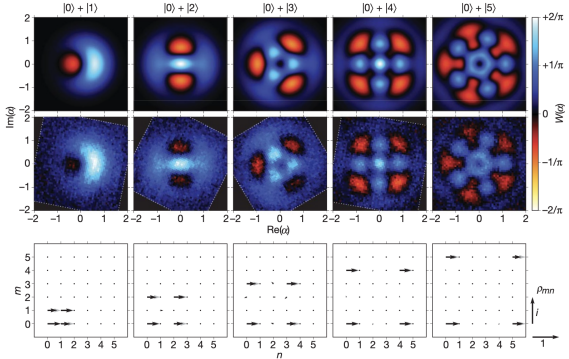

Figure 3 | Wigner tomography of superpositions of resonator Fock states $|0\rangle + |N\rangle$. The top row displays the theoretical form of the Wigner function $W(\alpha)$ as a function of the complex resonator amplitude α in photon number units, for states $N = 1$ to 5. The measured Wigner functions are shown in the middle row, with the colour scale bar on the far right. Negative quasi-probabilities are clearly measured. The experimental Wigner functions have been rotated to match theory, compensating for a phase delay between the qubit and resonator microwave lines; the measured area is bounded by a dotted white line. The bottom row displays the calculated (grey) and measured (black) values for the resonator density matrix ρ, projected onto the number states $\rho_{mn} = \langle m|\rho|n\rangle$. The magnitude and phase of ρ_{mn} is represented by the length and direction of an arrow in the complex plane (for scale, see key on right). The fidelities $F = \sqrt{\langle\psi|\rho|\psi\rangle}$ between the desired states $|\psi\rangle$ and the measured density matrices ρ are, from left to right, $F = 0.92$, 0.89, 0.88, 0.94 and 0.91. Each of the 51 by 51 pixels (61 by 61 for $N = 5$) in the Wigner function represents a local measurement. The value of $W(\alpha)$ is calculated at each pixel from 50 (41 for $N = 4$ and 5) interaction times τ, each repeated 900 times to give $P_e(\tau)$. This direct mapping of the Wigner function takes $\sim 10^8$ measurements or ~ 5 h.

Purcell filter for qubit readout

PHYSICAL REVIEW A **92**, 012325 (2015)

Quantum theory of a bandpass Purcell filter for qubit readout

Eyob A. Sete,[1,*] John M. Martinis,[2,3] and Alexander N. Korotkov[1]
[1]*Department of Electrical and Computer Engineering, University of California, Riverside, California 92521, USA*
[2]*Department of Physics, University of California, Santa Barbara, California 93106, USA*
[3]*Google Inc., Santa Barbara, California, USA*
(Received 22 April 2015; published 21 July 2015)

The measurement fidelity of superconducting transmon and Xmon qubits is partially limited by the qubit energy relaxation through the resonator into the transmission line, which is also known as the Purcell effect. One way to suppress this energy relaxation is to employ a filter which impedes microwave propagation at the qubit frequency. We present semiclassical and quantum analyses for the bandpass Purcell filter realized by E. Jeffrey *et al.* [Phys. Rev. Lett. **112**, 190504 (2014)]. For typical experimental parameters, the bandpass filter suppresses the qubit relaxation rate by up to two orders of magnitude while maintaining the same measurement rate. We also show that in the presence of a microwave drive the qubit relaxation rate further decreases with increasing drive strength.

DOI: 10.1103/PhysRevA.92.012325 PACS number(s): 03.67.Lx, 85.25.−j, 03.65.Yz

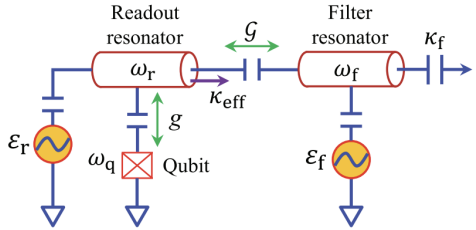

FIG. 2. (Color online) Qubit measurement schematic with the bandpass Purcell filter of Ref. [17]. The readout resonator with frequency ω_r (which depends on the qubit state) is coupled (coupling $\mathcal{G}$) with a filter resonator of frequency ω_f, which decays into the transmission line with the rate κ_f. The further processing of the outgoing microwave (not shown) is the same as in Fig. 1. The microwave drive can be applied either to the readout (ε_r) or to the filter (ε_f) resonators. Coupling with the decaying filter resonator produces an effective decay rate κ_{eff} of the readout resonator, which depends on the drive frequency. As a result, for the measurement microwave $\kappa_{eff} = \kappa_r$, while the qubit sees a much smaller value $\kappa_{eff} = \kappa_q$, thus leading to a suppression of the qubit Purcell decay by a factor κ_q/κ_r.

Paper for next week

Vol 445|1 February 2007|doi:10.1038/nature05461 nature

LETTERS

Resolving photon number states in a superconducting circuit

D. I. Schuster[1]*, A. A. Houck[1]*, J. A. Schreier[1], A. Wallraff[1]†, J. M. Gambetta[1], A. Blais[1]†, L. Frunzio[1], J. Majer[1], B. Johnson[1], M. H. Devoret[1], S. M. Girvin[1] & R. J. Schoelkopf[1]